ORIGINAL ARTICLE

The value of 18F-FDG PET/CT in Langerhans cell histiocytosis

Rongchen An[1] · Xiaowei Ma[1] · Yunhua Wang[1]

Abstract

Objective To investigate the value of 18F-FDG PET/CT in diagnosis and disease evaluation of Langerhans cell histiocytosis (LCH).

Methods A retrospective analysis of 31 patients with LCH confirmed by histopathology was performed. A systematic analysis of the PET/CT imaging manifestations of LCH was performed, recording patients who were treated and receiving PET/CT for efficacy evaluation. In addition, clinical and laboratory data of LCH patients were collected, and the correlation between these data and PET/CT metabolic parameters was initially investigated.

Results Of the 31 patients, thirty had at least 1 PET/CT positive lesions (96.7%), and one had only skin damage without abnormalities on PET/CT. Of 31 patients, fifteen (48.4%) had single system (SS) disease (9 cases with a single site and 6 cases with multiple sites) and 16 (51.6%) had multisystem (MS) disease (6 low risk and 10 high risk cases). The incidence of LCH lesions in the bone, lymphatic system, pituitary gland, liver, soft tissue, thyroid gland, thymus, and lungs was 20 cases (64.5%), 12 cases (38.7%), 3 cases (9.7%), 2 cases (6.5%), 2 cases (6.5%), 1 case (3.2%), 1 case (3.2%), and 8 cases (25.8%), respectively. A total of 21 PET/CT follow-up scanning were performed in 13 patients receiving chemotherapy, with 13 (61.9%) partial metabolic remission (PMR), 6 (28.6%) progressive metabolic disease (PMD), and 2 (9.5%) stable metabolic disease (SMD), according to PET Response Evaluation Criteria in Solid Tumors (PRECIST) 1.0. Erythrocyte sedimentation rate (ESR), C-reactive protein (CRP) and Lactic Dehydrogenase (LDH) were positively correlated with TTLG (total TLG) ($R^2 = 0.3256, 0.2409, 0.4205, P < 0.05$). The Re-examine SUVmax is positively correlated with re-examine LDH ($R^2 = 0.7285, P < 0.05$).

Conclusions 18F-FDG PET/CT is an effective way to diagnose and evaluate LCH. PET metabolic parameters were associated with laboratory inflammatory markers, suggesting that 18F-FDG PET/CT may be helpful in evaluating disease activity of LCH.

Keywords Langerhans cell histiocytosis · 18F-fluorodeoxyglucose · PET/CT · Disease Activity

Introduction

Langerhans cell histiocytosis (LCH) is an inflammatory myeloid neoplasm characterized by the clonal proliferation and accumulation of pathological Langerhans cells in various organs or systems. In LCH, patients with mild cases present as isolated, painless bone lesions, while severe cases exhibit extensive organ infiltration accompanied by fever and weight loss [1]. The current classification system is based on the location and number of lesions (Single system: single site and multiple sites. Multisystem: with or without risk organ involvement). In recent years, 18F-FDG PET/CT has also been reported in some individual and small case series, but it has yielded some contradictory or inconclusive results [2–9]. Due to the potential involvement of multiple organs in LCH, PET/CT may be superior to traditional imaging in detecting these lesions and evaluating treatment effect.

The hallmark of LCH is robust immune infiltration, even though the mechanisms are not clear. The pathologic CD207+ dendritic cells make up a median of 8% of LCH lesion cells, with the rest composed of inflammatory infiltrates [10]. In addition, some LCH patients may experience fever, which can result in elevated laboratory results such as ESR and CRP. Therefore, the development of new tools to

✉ Yunhua Wang
  wangyunhua0801@csu.edu.cn

1 Department of Nuclear Medicine, The Second Xiangya Hospital, Central South University, 139# Renmin Middle Road Changsha, Changsha 410011, Hunan, China

effectively monitor disease activity is crucial in preventing LCH recurrence or reactivation.

We hypothesize that the metabolic parameters of 18F-FDG PET/CT are correlated with these inflammatory markers. In this study, we conducted a retrospective survey of a group of LCH patients and performed semiquantitative analysis of the imaging features and metabolic characteristics of LCH patients. We also made an initial exploration of the role of 18F-FDG PET/CT in assessing disease activity.

Materials and methods

Patient baseline data

From March 2014 to December 2022, a retrospective analysis was conducted on 31 LCH patients who underwent 18F-FDG PET/CT scans. 31 scans were used for initial staging, and 21 scans were used for restaging or follow-up. PET/CT scans are completed within 1 month after chemotherapy. Use the PET Response Evaluation Criteria in Solid Tumors (PRECIST) 1.0 to evaluate the efficacy of follow-up or restaging patients [11]. This study is in line with the principles of the Declaration of Helsinki.

Conventional imaging

Conventional imaging includes X-rays, computer tomography (CT), and magnetic resonance imaging (MRI). Before treatment, 31 patients received a total of 56 non-PET /CT scans for diagnosis and staging: 13 X-rays scans, 24 CT scans, and 19 MRI scans.

^{18}F-FDG PET/CT image acquisition

The imaging was performed by Siemens Biograph mCTx PET/CT. 18F was prepared by Siemens cyclotron and 18F-FDG was synthesized by Explora FDG4 and Explora GN chemical synthesis modules with radiochemical purity > 95%. Before injection of 18F-FDG, the patient routinely fasted for more than 6 h, and the blood glucose was < 11.1 mmol/L. The injection dose was 3.7 MBq/kg and was injected into the patient via an elbow vein. PET/CT scans were performed 60 min after injection, ranging from the roof of the skull to the middle thigh. Low-dose CT acquisition followed by PET. Low dose CT voltage: 120 kV, automatic milliampere second, matrix 512×512, layer thickness 5 mm. Each bed was scanned for 2 min, and 5–6 beds were collected.

PET/CT image analysis

PET/CT imaging was firstly visually analyzed by two experienced nuclear medicine physicians (Dr. Wang and Dr. Ma) to determine whether there was abnormal 18F-FDG uptake and/or structural changes in the imaging. Focal tracer uptake higher than physiological distribution and background are considered positive lesions. We used software (MEDEX) that defines the PET-based lesion contour with a cut-off value of 41% of the tumoral maximum standardized uptake value (SUVmax) and provides the following parameters: SUVmax, metabolic tumor volume (MTV), total lesion glycolysis (TLG), total MTV (TMTV) and total TLG (TTLG). The region of interest (ROI) of different shapes was used to completely wrap the lesions. TMTV and TTLG were calculated as the sums of the MTV and TLG of all lesions of each patient.

Statistical analysis

All statistical analysis was carried out using the Statistical Package for the Social Sciences (SPSS) version 26.0 (IBM, Chicago, IL, USA). Quantitative data were represented by mean $\pm$ standard deviation ($\bar{x} \pm s$), minimum and maximum. Pearson correlation analysis was used to analyze the correlation between clinical parameters and PET metabolic parameters. Paired sample t-test was used to compare the difference of PET metabolic parameters before and after chemotherapy, and $P < 0.05$ was statistically significant.

Results

Study population and cohort data

From March 2014 to December 2022, a total of 31 patients with LCH underwent 18F-FDG PET/CT scan, including 18 men and 13 women (Table 1). There were 4 patients < 18 years old and 27 patients ≥ 18 years old. 20 patients were confirmed by biopsy, and 11 patients were confirmed by surgery. Of the 31 patients, fifteen (46.9%) had SS disease (single lesion: 9, multiple lesions: 6), and 16 (53.1%) had MS disease (low risk: 6, high risk: 10). All patients underwent 18F-FDG PET/CT scans before treatment. Thirteen patients underwent at least one PET/CT scan after treatment, including 8 cases with 1scan, 3 cases with 2 scans, 1 case with 3 scans, and 1 case with 4 scans. Six patients were tested for the BRAF-V600E gene, including five wild-type and one mutant.

Table 1 Baseline characteristics of LCH patients

Variables	n	Minimum	Maximum	$\bar{x} \pm s$
WBC count (/μL)	31	4.3	18.8	7.5±2.8
RBC count (/μL)	31	2.3	5.7	4.6±0.7
Platelet count (1000/μL)	31	118.0	664.0	279.0±110.3
Hemoglobin (g/dL)	31	63.0	174.0	132.2±21.1
Neutrophil count (/μL)	31	2.1	15.6	5.0±2.4
Monocyte count (/μL)	31	0.2	0.8	0.4±0.2
Lymphocyte count (/μL)	31	0.7	6.9	1.8±1.1
ALT (IU/L)	31	5.0	150.3	31.7±35.5
AST (IU/L)	31	13.8	157.4	28.2±25.2
ESR (mm/h)	15	9.0	120.0	47.3±34.8
CRP (mg/L)	18	0.1	89.2	24.6±23.5
LDH (IU/L)	23	117.0	777.8	293.2±169.6

WBC white blood cell, *RBC* red blood cell, *ALT* alanine aminotransferase, *AST* aspartate aminotransferase, *ESR* erythrocyte sedimentation rate, *CRP* C-reactive protein, *LDH* lactate dehydrogenase

18F-FDG PET/CT imaging findings

The positive rate of PET/CT was 96.8%(30/31), showing at least one hypermetabolic lesion consistent with LCH. The main manifestations were increased uptake of 18F-FDG in bone, lymph systems and other organs and tissues. There were 397 lesions in 30 patients (except lung lesions).

Bone involvement

Twenty patients (67.7%) had bone lesions (Fig. 1, Table 2). The spine is the most affected site, including 163 osteolytic lesions (two without metabolism), twelve osteoblastic lesions (two without metabolism), and 3 mixed lesions. In 6 bone lesions, there was no density change on conventional X-ray or CT.

Lymphatic system involvement

Eleven patients had lymph node lesions (Fig. 1). The diseased lymph nodes were distributed in the whole body, including head and neck, mediastinum and hilum of lung, cardiophrenic angle, axilla, retroperitoneum, abdominal cavity, and groin region. The spleen was involved in a patient, including two highly active lesions (a lesion with decreased density and another with no density change). The thymus was involved in a patient, presenting as anterior mediastinal masses with significantly increased activity.

Pituitary involvement

Four patients (12.9%) had pituitary involvement. Three patients showed pituitary thickening or sellar region nodules with increased metabolism, and one patient showed obvious flattening of pituitary gland without FDG uptake.

Liver lesions

Two patients (6.5%) had liver involvement. Both patients presented with hepatomegaly with multiple low-density nodules in the liver. At the same time, 18F-FDG uptake was increased.
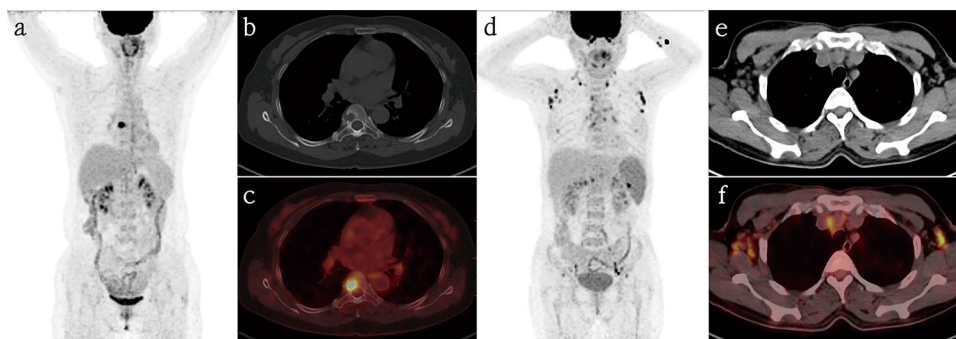

Fig. 1 18F-FDG PET/CT findings of bones and lymph nodes involvement in LCH patients. **a-c** were the images of a 54-year-old woman. Maximal intensity projection (MIP) **a** showed abnormal uptake of 18F-FDG in the spine, and CT bone window **b** and PET/CT fused images **c** showed osteolytic destruction of the T8 vertebral body with increased metabolism (SUVmax:15.8). In a 49-year-old woman, MIP **d** showed multiple 18F-FDG uptake in the neck, mediastinum, and axilla, and CT **e** and PET/CT **f** showed multiple slightly enlarged lymph nodes in the bilateral axilla and mediastinum with increased activity (SUVmax:9.8)

Table 2 Summary of the anatomical distribution of LCH lesions

Anatomical sites	Number		SUVmax	
	No. of patients	No. of lesions	$\bar{x} \pm s$	Range
Bone	20	184	12.8 ± 5.7	2.0–24.9
Skull	7	17	7.5 ± 4.7	1.9–14.8
Scapula	2	5	13.3 ± 7.1	6.2–20.3
Sternum	4	6	10.7 ± 8.5	3.3–24.9
Ribs	5	27	9.6 ± 3.8	5.1–15.7
Column	10	48	13.3 ± 4.2	5.4–18.1
Pelvis	7	60	12.0 ± 5.3	5.4–19.5
Extremities	6	21	7.4 ± 2.0	3.5–9.0
Extra skeletal	16	213	11.9 ± 10.6	3.6–44.5
Lymph nodes	11	129	8.1 ± 4.4	3.6–17.2
Pituitary	3	3	25.4 ± 16.7	3.9–44.7
Liver	2	67	9.5 ± 1.5	8.0–10.5
Soft tissue	2	10	6.9 ± 1.0	5.9–7.8
spleen	1	2	6.7 ± 0.4	6.1–7.2
Thyroid	1	1	35.6	35.6
Thymus	1	1	16.0	16.0
Lung*	7	np	2.9 ± 1.9	0.9–7.5

No. number * The evaluation of the number of lungs LCH lesions was not performed because they have particular morphological patterns of presentation (multinodular or cystic)

Soft tissue lesions

Two patients (6.5%) had soft tissue involvement. This included a case of muscle swelling with increased 18F-FDG and a case of localized increased metabolism in the right intercostal pleura (no abnormalities in morphology and density on CT).

Thyroid lesions

A patient (3.2%) had thyroid involvement, characterized by abnormal thyroid tumescence with increased activity (Fig. 2).

Pulmonary lesions

Eight male patients (25.8%) had lung involvement. The mean age was 37 years, six patients had a history of smoking (all were smoking), and two patients had no history of smoking. Of the eight patients with pulmonary LCH, two patients presented with small or miliary nodules, four patients presented with cystic lesions and nodules, a patient only presented with cystic lesions, and a patient presented with patchy high-density and ground glass shadows (Fig. 2). 7 patients were accompanied by increased 18F-FDG uptake.

PET/CT vs. conventional imaging

Thirteen patients underwent at least one PET/CT scan before and after treatment (a total of 21 scans, Table 3). According to PERCIST 1.0, partial metabolic remission (PMR) accounted for 61.9%(13/21), partial metabolic progression

Fig. 2 18F-FDG PET/CT findings of thyroid and lungs involvement in LCH patients. In a 59-year-old woman, MIP **a** showed abnormal uptake of 18F-FDG in the neck, and PET/CT fused images in coronal **b** and sagittal **c** showed significant enlargement of both thyroid lobes with diffuse metabolic abnormalities (SUVmax: 44.7). In another 57-year-old man, MIP **d** showed increased diffuse 18F-FDG uptake in the chest, and CT **e** and PET/CT fused images **f** showed multiple ground glass shadows and solid shadows with elevated metabolism (SUVmax: 9.2)
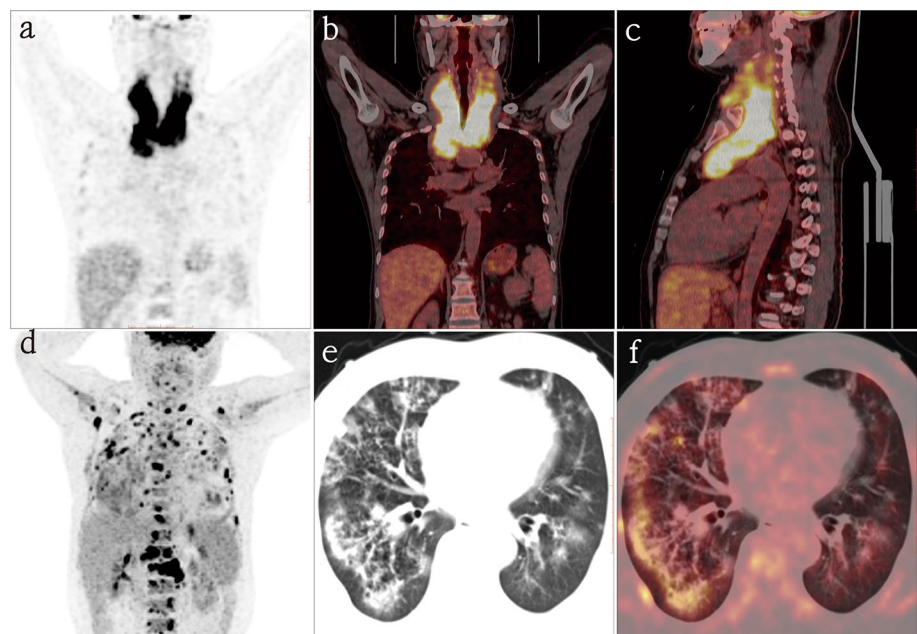
Table 3 Evaluation of curative effect of 13 patients with LCH

Patients	Group	Therapy	Evaluation by PERCIST 1.0			
			First	Second	Third	Fourth
1	SS, single site	Chemotherapy	PMR	–	–	–
2	SS, multiple sites	Chemotherapy	PMR	PMR	PMD	PMD
3	SS, multiple sites	Chemotherapy	PMD	–	–	–
4	SS, multiple sites	Chemotherapy	PMR	–	–	–
5	SS, multiple sites	Chemotherapy	SMD	–	–	–
6	MS, High-risk	Chemotherapy	PMR	–	–	–
7	MS, Low risk	Chemotherapy	PMD	PMR	–	–
8	MS, High-risk	Chemotherapy	PMR	–	–	–
9	MS, Low risk	Chemotherapy	PMR	PMD	PMR	–
10	MS, High-risk	Chemotherapy	PMD	–	–	–
11	MS, Low-risk	Chemotherapy	PMR	PMR	–	–
12	MS, High-risk	Chemotherapy	PMR	–	–	–
13	MS, Low risk	Chemotherapy	SMD	PMR	–	–

LCH langerhans cell histiocytosis, *PERCIST* PET response evaluation criteria in solid tumors, *PMD* progressive metabolic disease, *PMR* partial metabolic response, *SMD* stable metabolic disease, *SS* single system, *MS* multisystem

(PMD) for 28.6%(6/21), and stable metabolic disease (SMD) for 9.5%(2/21). Eighteen patients did not receive PET/CT follow-up. For PMR group, SUVmax after treatment was significantly lower than that before treatment $(15.762 \pm 15.971$ vs 9.910 ± 12.584, $t = 3.110$, $P = 0.009)$. For PMD group, SUVmax after treatment was significantly higher than that before treatment $(10.699 \pm 15.796$ vs 15.453 ± 19.743, $t = 2.776$, $P = 0.039)$. For SMD group, there was no significant difference between SUVmax after treatment and before treatment $(21.504 \pm 18.082$ vs 23.763 ± 11.807, $t = 0.509$, $P = 0.700)$.

Association of laboratory variables with metabolic parameters

In 30 LCH patients with positive lesions on PET/CT, ESR, CRP and LDH were positively correlated with TTLG

Fig. 3 ESR, CRP and LDH correlated positively with TTLG ($P < 0.05$), re-examine LDH correlated positively with re-examine SUVmax ($P < 0.05$). *ESR* erythrocyte sedimentation rate, *CRP* C-reactive protein, *LDH* lactate dehydrogenase, *TTLG* total TLG, *SUVmax* maximum standardized uptake value
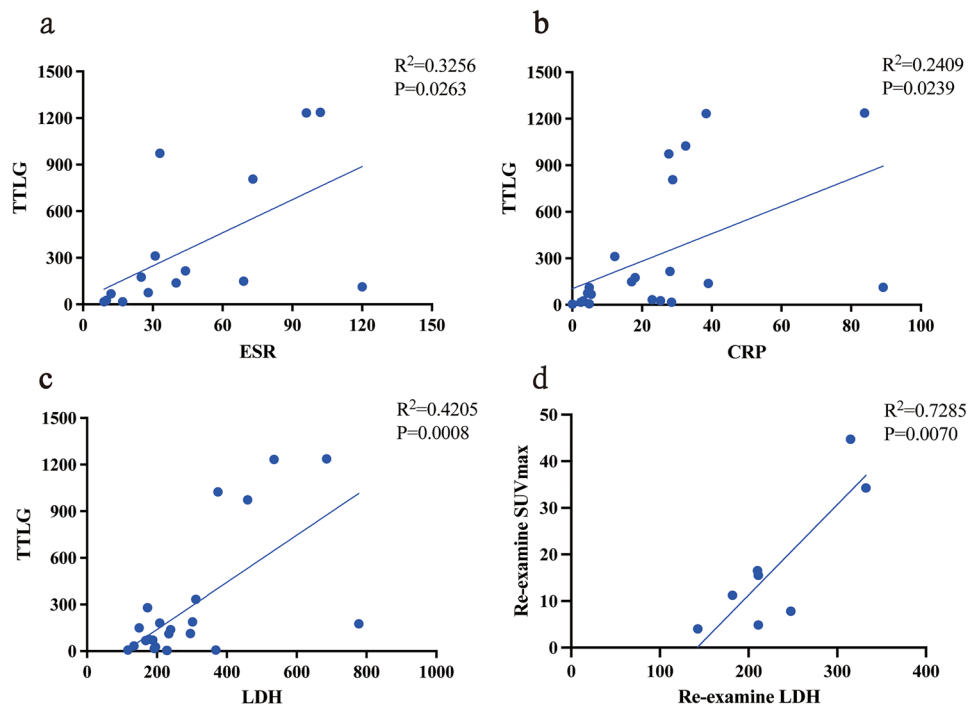
($R^2 = 0.3256$, 0.2409, 0.4205, $P = 0.0263$, 0.0239, 0.0008, Fig. 3). There were no significant differences in metabolic parameters and clinical indexes between SS-LCH and MS-LCH. Eight patients underwent both LDH and PET/CT re-examine after treatment. The re-examine LDH were positively correlated with the re-examine SUVmax ($R^2 = 0.7285$, $P = 0.0070$).

Discussions

LCH is an inflammatory myeloid neoplasm. Langerhans cells are named after Paul Langerhans, who first reported in 1868. Langerhans cells are dendritic cells. The physiologic function of dendritic cells is to interact with and activate T cells, and LCH lesions are characterized by a robust immune infiltrate, although mechanisms driving inflammation are not well understood [10]. In LCH lesions, the pathologic dendritic cells constitute less than 1% to more than 70% of the granulomatous lesion (median, approximately 8%) [12]. The remainder of the lesion is composed of inflammatory infiltrate, including activated T cells on the background of a cytokine storm [13–15]. We provide a brief overview of the 18F-FDG PET/CT findings in LCH across various systems and attempt to explore the correlation between PET metabolic parameters and laboratory parameters.

First, we found that most lesions took up 18F-FDG. PET/CT contributes to the diagnosis and assessment of therapeutic effectiveness in LCH, with higher sensitivity compared to conventional imaging, consistent with previous reports [16–18]. Bones are the most affected sites in LCH [19]. Based on PET/CT imaging, some early lesions may exhibit metabolic abnormalities without morphological changes. Our study also identified several lesions with increased 18F-FDG uptake alone. This unique advantage of PET/CT is valuable in diagnosing clinically asymptomatic lesions with no routine radiological abnormalities. The lymphatic system is also one of the most involved sites, primarily including lymph nodes, thymus, and spleen [17, 20]. Lymph node involvement is usually a part of systemic LCH and is characterized by lymph node enlargement with increased 18F-FDG uptake. Like lymph nodes, involvement of organs such as the liver, spleen, and soft tissues is nonspecific. As a whole-body examination, PET/CT, when combined with clinical and laboratory information, aids in arriving at possible diagnoses and improving the accuracy of diagnosing involvement of certain organs and systems.

Our study for the first time revealed a positive correlation between ESR, CRP, LDH, and TTLG of LCH lesions. Similarly, post-treatment Re-examine LDH was positively correlated with Re-examine SUVmax. These results may suggest that PET/CT can assess LCH disease activity. SUVmax reflects the highest local 18F-FDG metabolic activity within the lesion and is often positively associated with the invasiveness of the tumor. TLG, based on MTV, is a comprehensive parameter representing tumor metabolic activity and metabolic volume, which helps determine the glucose load of the lesion site [21]. TTLG, as an indicator of the overall tumor burden, more accurately reflects the patient's tumor burden. Aerobic glycolysis is (AG) considered a hallmark of tumor initiation and progression [22]. LDH, as a key enzyme in AG, is abnormally overexpressed in many malignant tumors and is associated with tumor growth, maintenance, and invasion [23, 24]. This can explain the correlation between LDH and SUVmax and TTLG. CRP is a highly sensitive systemic marker of inflammation and tissue damage, while ESR is a non-specific biomarker influenced by both inflammatory and non-inflammatory factors [25]. Since inflammatory infiltrate makes up a significant portion of LCH lesions, this may lead to an elevation in ESR and CRP.

Our results indicate that TMTV is not correlated with inflammatory markers, possibly due to limitations in the measurement method. Like most previous studies, MTV, TLG, TMTV, and TTLG were computed using a fixed SUVmax threshold of 40%–50% [26, 27]. This threshold method has limitations in measuring lesion activity and volume. Other authors have used a fixed SUV threshold, most commonly 2.5, with the obvious limitations of an arbitrary cutoff [28]. Therefore, our future work will draw inspiration from Burger et al.'s PET volume metrics based on background-adaptive methods [29].

Our study has several limitations. Firstly, being a retrospective study may lead to patient selection bias. Secondly, only a subset of patients underwent PET/CT for therapeutic evaluation, which could underestimate the advantages of PET/CT. As discussed in the paper, using fixed thresholds may not accurately detect tumor activity and volume. Lastly, the rarity of LCH results in a relatively small sample size, particularly for those who underwent clinical and PET/CT follow-up. Therefore, the findings obtained still require validation with large multicenter datasets.

In summary, our study suggests that PET/CT assessment is valuable for LCH, with higher sensitivity compared to conventional imaging modalities. The results of the correlation analysis indicate that PET/CT may be an effective method for evaluating the disease activity of LCH.

Conclusion

In summary, our study shows that PET/CT is useful for evaluating LCH, with higher sensitivity than conventional imaging. PET/CT may be an effective way to assess disease activity for LCH, which is helpful for personalized-management of LCH.

Data availability All relevant data are within the paper.

Declarations

Conflict of interest The authors declare that they have no conflict of interest.

Human and animal Not applicable.

Ethical approval Not applicable.

Consent for participating and for publication Patients signed an informed consent to participate and to use their anonymous data for analysis and publication of results.

Consent informed Not applicable.

References

1. Allen CE, Merad M, McClain KL. Langerhans-cell histiocytosis. N Engl J Med. 2018;379(9):856–68.
2. Binkovitz LA, Olshefski RS, Adler BH. Coincidence FDG-PET in the evaluation of Langerhans' cell histiocytosis: preliminary findings. Pediatr Radiol. 2003;33(9):598–602.
3. Kaste SC, Rodriguez-Galindo C, McCarville ME, Shulkin BL. PET-CT in pediatric Langerhans cell histiocytosis. Pediatr Radiol. 2007;37(7):615–22.
4. Phillips M, Allen C, Gerson P, McClain K. Comparison of FDG-PET scans to conventional radiography and bone scans in management of Langerhans cell histiocytosis. Pediatr Blood Cancer. 2009;52(1):97–101.
5. Lee HJ, Ahn BC, Lee SW, Lee J. The usefulness of F-18 fluorodeoxyglucose positron emission tomography/computed tomography in patients with Langerhans cell histiocytosis. Ann Nucl Med. 2012;26(9):730–7.
6. Zhou W, Wu H, Han Y, Wang S, Dong Y, Wang Q. Preliminary study on the evaluation of Langerhans cell histiocytosis using F-18-fluorodeoxy-glucose PET/CT. Chin Med J (Engl). 2014;127(13):2458–62.
7. Garcia JR, Riera E, Bassa P, Mourelo S, Soler M. (18)F-FDG PET/CT in follow-up evaluation in pediatric patients with Langerhans histiocytosis. Rev Esp Med Nucl Imagen Mol. 2017;36(5):325–8.
8. Zhao Y, Zhou Y, Tian R, Su M. Solitary bone Langerhans cell histiocytosis demonstrated on multimodality imaging in an adult. Clin Nucl Med. 2020;45(1):78–80.
9. Xu T, Cen B, Li H, Wang Y, Chen Y. 99m Tc-MDP bone scan findings of recurrent Langerhans cell histiocytosis in an adult involving femur after joint replacement. Clin Nucl Med. 2023;48(9):804–5.
10. Rodriguez-Galindo C, Allen CE. Langerhans cell histiocytosis. Blood. 2020;135(16):1319–31.
11. Pinker K, Riedl C, Weber WA. Evaluating tumor response with FDG PET: updates on PERCIST, comparison with EORTC criteria and clues to future developments. Eur J Nucl Med Mol Imaging. 2017;44(Suppl 1):55–66.
12. Berres ML, Lim KP, Peters T, Price J, Takizawa H, Salmon H, et al. BRAF-V600E expression in precursor versus differentiated dendritic cells defines clinically distinct LCH risk groups. J Exp Med. 2014;211(4):669–83.
13. Laman JD, Leenen PJ, Annels NE, Hogendoorn PC, Egeler RM. Langerhans-cell histiocytosis "insight into DC biology." Trends Immunol. 2003;24(4):190–6.
14. Senechal B, Elain G, Jeziorski E, Grondin V, Patey-Mariaud de Serre N, Jaubert F, et al. Expansion of regulatory T cells in patients with Langerhans cell histiocytosis. PLoS Med. 2007;4(8):e253.
15. Allen CE, Li L, Peters TL, Leung HC, Yu A, Man TK, et al. Cell-specific gene expression in Langerhans cell histiocytosis lesions reveals a distinct profile compared with epidermal Langerhans cells. J Immunol. 2010;184(8):4557–67.
16. Wang J, Song T, Wang J, Ma L, Jiang Y, Kong D, et al. Aggressive Langerhans cell histiocytosis transformation of T cell acute lymphoblastic leukemia detected on (18)F-FDG PET/CT. Eur J Nucl Med Mol Imaging. 2021;48(2):642–3.
17. Luo ZH, Lu PX, Qi WL, Liao FX, Jin AF, Zen QY. Role of (18) F-FDG PET/CT in the diagnosis and management of patients with Langerhans cell histiocytosis. Quant Imaging Med Surg. 2022;12(6):3351–63.
18. Albano D, Bosio G, Giubbini R, Bertagna F. Role of (18)F-FDG PET/CT in patients affected by Langerhans cell histiocytosis. Jpn J Radiol. 2017;35(10):574–83.
19. Kobayashi M, Ando S, Kawamata T, Makiyama J, Yokoyama K, Imai Y, et al. Clinical features and outcomes of adult Langerhans cell histiocytosis: a single-center experience. Int J Hematol. 2020;112(2):185–92.
20. Agarwal KK, Seth R, Behra A, Jana M, Kumar R. 18F-Fluorodeoxyglucose PET/CT in Langerhans cell histiocytosis: spectrum of manifestations. Jpn J Radiol. 2016;34(4):267–76.
21. Ohshima K, Fujiya K, Nagashima T, Ohnami S, Hatakeyama K, Urakami K, et al. Driver gene alterations and activated signaling pathways toward malignant progression of gastrointestinal stromal tumors. Cancer Sci. 2019;110(12):3821–33.
22. Gatenby RA, Gillies RJ. Why do cancers have high aerobic glycolysis? Nat Rev Cancer. 2004;4(11):891–9.
23. McCleland ML, Adler AS, Deming L, Cosino E, Lee L, Blackwood EM, et al. Lactate dehydrogenase B is required for the growth of KRAS-dependent lung adenocarcinomas. Clin Cancer Res. 2013;19(4):773–84.
24. de la Cruz-Lopez KG, Castro-Munoz LJ, Reyes-Hernandez DO, Garcia-Carranca A, Manzo-Merino J. Lactate in the regulation of tumor microenvironment and therapeutic approaches. Front Oncol. 2019;9:1143.
25. Pepys MB, Hirschfield GM. C-reactive protein: a critical update. J Clin Invest. 2003;111(12):1805–12.
26. Zer A, Domachevsky L, Rapson Y, Nidam M, Flex D, Allen AM, et al. The Role of 18F-FDG PET/CT on staging and prognosis in patients with small cell lung cancer. Eur Radiol. 2016;26(9):3155–61.
27. Kwon HR, Cho J, Park S, Lee SH, Ahn MJ, Choi JY, et al. Metabolic parameters on baseline (18)F-FDG PET/CT are potential predictive biomarkers for immunotherapy in patients with head and neck squamous cell carcinoma. Front Med (Lausanne). 2022;9: 896494.
28. Lee JW, Kang CM, Choi HJ, Lee WJ, Song SY, Lee JH, et al. Prognostic value of metabolic tumor volume and total lesion glycolysis on preoperative (1)(8)F-FDG PET/CT in patients with pancreatic cancer. J Nucl Med. 2014;55(6):898–904.
29. Burger IA, Casanova R, Steiger S, Husmann L, Stolzmann P, Huellner MW, et al. 18F-FDG PET/CT of non-small cell lung

carcinoma under neoadjuvant chemotherapy: background-based adaptive-volume metrics outperform TLG and MTV in predicting histopathologic response. J Nucl Med. 2016;57(6):849–54.